RADIO SCIENCE Journal of Research NBS/USNC–URSI
Vol. 68D, No. 3, March 1964

A Simplified Theory of Diffraction at an Interface Separating Two Dielectrics

Julius Kane[1] and Samuel N. Karp[2]

(Received October 25, 1963)

Many electromagnetic problems involving more than one dielectric medium are not susceptible of an exact solution, when the appropriate boundary conditions are considered. The purpose of the present paper is to formulate a new boundary condition, which is capable of leading to mathematically tractable problems, with limited sacrifices in accuracy.

1. Introduction

The theoretical treatments of mixed-path propagation [Wait, 1962a] problems usually depend upon the introduction of a Leontovich, or impedance type boundary condition which specifies the ratio of tangential $\vec{E}$ and $\vec{H}$ to characterize ground conductivity. Otherwise, if one attempts to match tangential $\vec{E}$ and $\vec{H}$ across an interface, as required by the rigorous theory, then intractable boundary value problems usually arise. As a result, the use of linear boundary conditions to model the physics at an interface is virtually required, if numerical results are desired. However, the Leontovich boundary condition is known to represent the phenomena well only if the ground conductivity is high, in which case the surface impedance is reasonably independent of the angle of incidence. That is, if the ground has low losses, or is a fairly good dielectric, then there is significant penetration into this medium, and higher order boundary conditions are required if the physics at the interface is to be modeled accurately. It is the purpose of this note to introduce a more accurate version of the Leontovich boundary condition for use in propagation problems involving dielectric interfaces.

2. Construction of the Boundary Condition

In our search for a boundary condition that reproduces the phenomenology of transition conditions at dielectric interfaces we have been motivated by the form of solutions to some radiation problems. The standard two-media problem of a radiating line source above a dielectric interface yields a secondary field or diffraction contribution, represented by an integral of the form

$$\int_C R(\phi)\, e^{ik_1\rho\cos(\phi-\psi)}\, d\phi,$$

in addition to the free space Green's function. In the integral $R(\phi)$ is the appropriate Fresnel reflection coefficient for the dielectric interface, and the contour C is the familiar path defining the Hankel function. The diffracted field has the interpretation of a summation of plane waves, traveling in all directions, real and imaginary, which have as a weight factor *the Fresnel reflection coefficient* extended to the complex ϕ-plane. This suggests that the scattered field in the dielectric half space containing the source is characterized by the interface's *reflection* properties.

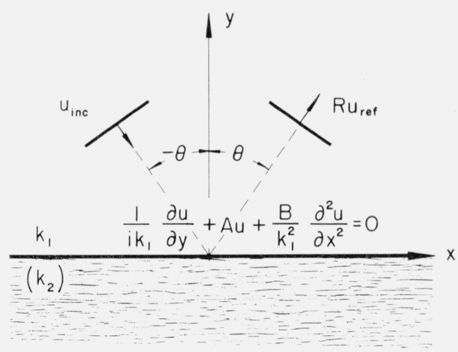

FIGURE 1. *The reflected fields for both the two-media problem and its reformulated counterpart have the same functional form and differ only in the value of the reflection coefficient* R.

When medium k_2 is *almost* conducting it is known that an impedance type boundary condition of the form [Grunberg, 1943; Leontovich, 1944]

$$\frac{\partial u}{\partial y}+\lambda u=0, \tag{1}$$

represents the phenomena fairly well. Therefore, for a more involved situation we seek to construct a higher order boundary condition with additional coefficients so as to match the Fresnel reflection coefficient. We start by noting that the boundary condition

$$\frac{1}{ik_1}\frac{\partial u}{\partial y}+Au+\frac{B}{k_1^2}\frac{\partial^2 u}{\partial x^2}u=0, \qquad y=0, \tag{2}$$

[1] University of Rhode Island, Kingston, R.I.
[2] Division of Electromagnetic Research, New York University, 25 Waverly Place, New York, N.Y.

imposed upon the wave equation

$$\nabla^2 u + k_1^2 u = 0, \qquad y \geq 0,\ k_1 = \frac{\omega}{c}, \tag{3}$$

implies plane wave solutions of the form (fig. 1)

$$u = u_{\text{inc}} + R_A(\theta) u_{\text{ref}},$$

where

$$u_{\text{inc}} = e^{ik_1(x \cos \theta - y \sin \theta)},$$

$$u_{\text{ref}} = e^{ik_1(x \cos \theta + y \sin \theta)},$$

provided that the reflection coefficient $R_A(\theta)$ is chosen as

$$R_A(\theta) = \frac{\cos \theta - (A - B \sin^2 \theta)}{\cos \theta + (A - B \sin^2 \theta)}. \tag{4}$$

An approximation procedure is evident: find A and B such that $R_A(\theta)$ is a suitable approximation to the Fresnel reflection coefficient appropriate for the polarization of the excitation field. We emphasize that the reflection coefficient in (4) is an approximating version of the Fresnel reflection coefficient by using the subscript A. For transverse electric excitation $u(x, y)$ represents E_z, $E_x = E_y = 0$; and the correct Fresnel coefficient is [Stratton, 1941],

$$R_{\text{TE}}(\theta) = \frac{\cos \theta - n \left[1 - \frac{1}{n^2} \sin^2 \theta\right]^{\frac{1}{2}}}{\cos \theta + n \left[1 - \frac{1}{n^2} \sin^2 \theta\right]^{\frac{1}{2}}}. \tag{5}$$

The geometry is that of figure 1, and $n = k_2/k_1$, is the index of refraction where k_2 is the propagation constant in the lower half space. For transverse magnetic excitation $u(x, y) = H_z$, $H_x = H_y = 0$; the reflection coefficient is

$$R_{\text{TM}}(\theta) = \frac{\cos \theta - \frac{1}{n} \left[1 - \frac{1}{n^2} \sin^2 \theta\right]^{\frac{1}{2}}}{\cos \theta + \frac{1}{n} \left[1 - \frac{1}{n^2} \sin^2 \theta\right]^{\frac{1}{2}}}. \tag{6}$$

For convenience only, we have assumed the magnetic permeabilities μ_1 and μ_2 of the two media to be identical. A comparison of $R_{\text{TE}}(\theta)$ and $R_{\text{TM}}(\theta)$ with (4) shows that we can approximate them for *all* real angles of incidence by picking A and B properly. To make this selection, we choose

$$\left.\begin{aligned} A_{\text{TE}} &= \frac{k_2}{k_1} = n \\ A_{\text{TM}} &= \frac{k_1}{k_2} = \frac{1}{n} \end{aligned}\right\}, \tag{7}$$

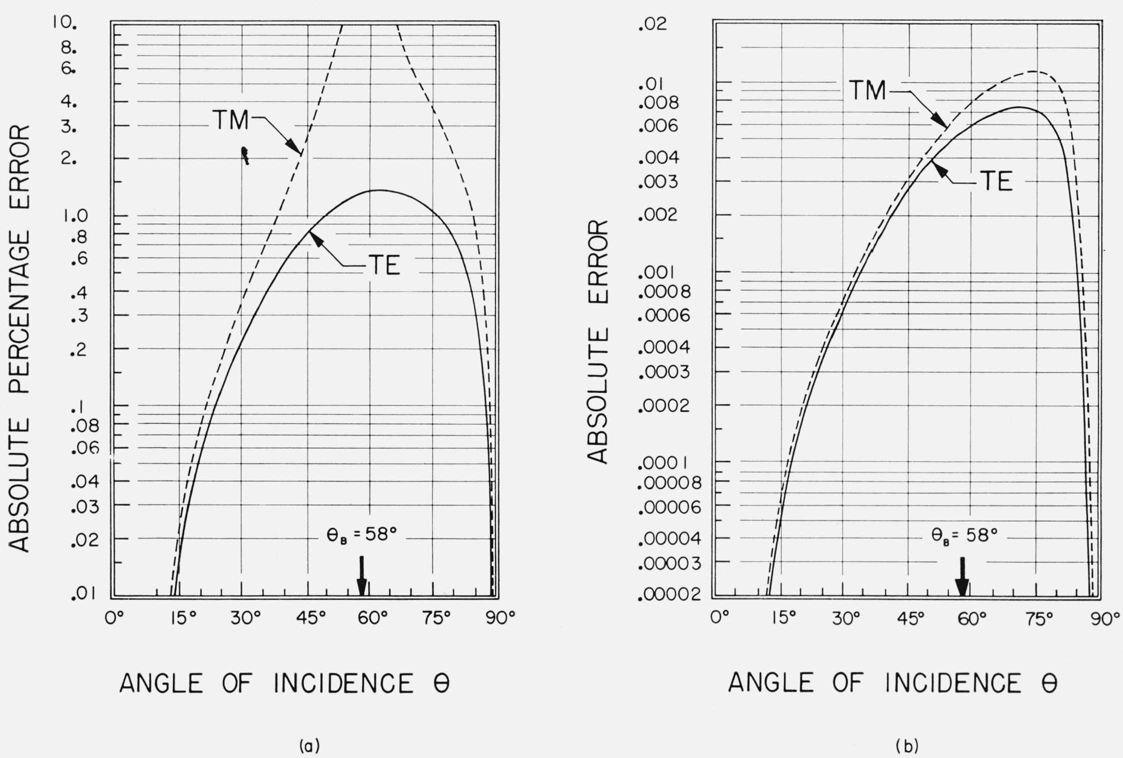

Graph No. 1.

The absolute percentage errors and the absolute errors that arise between the Fresnel reflection coefficients (5) and (6), and their approximations (4).

The curves are plotted as a function for θ for the index of refraction $n = 1.6$. In this case $B(\theta_e)$ has been chosen to make the match exact for $\theta_e = 0°$, or normal incidence.

so that the approximation (4) will agree exactly with either (5) or (6) for normal incidence ($\theta=0$). For glancing incidence ($\theta=\pm\pi/2$), the expression (4) will agree with (5) or (6) regardless of the choice of A or B since the *forms* of (4), (5), and (6) are such that all are equal to -1 for $\theta=\pm\pi/2$.

Having motivated a choice of the constant A, we shall devote the next few subsections to selection of the remaining constant B, which can be chosen in many useful ways.

2.1. General Angular Matching

The constant B in (4) above may be used to make $R_A(\theta)$ *exact* for some additional angle θ_e, where $0\leq\theta_e\leq\pi/2$. For any choice of θ_e, the $B_{\mathrm{TM,\,TE}}(\theta_e)$'s are determined by matching

$$1-\frac{B_{\mathrm{TE,\,TM}}}{A_{\mathrm{TE,\,TM}}}\sin^2\theta_e \text{ with } \left[1-\frac{1}{n^2}\sin^2\theta_e\right]^{1/2}$$

where $n=k_2/k_1$ is the index of refraction; inverting for $B_{\mathrm{TE,\,TM}}$ we find

$$B_{\mathrm{TE,\,TM}}(\theta_e)=\frac{A_{\mathrm{TE,\,TM}}\left\{1-\left[1-\frac{1}{n^2}\sin^2\theta_e\right]^{1/2}\right\}}{\sin^2\theta_e}. \tag{8}$$

Observe that choosing θ_e is equivalent to specifying $B_{\mathrm{TE,\,TM}}$.

2.2. Normal Matching

If $n>1$, we can expand the radical in (8) by the binomial theorem, and use the A's defined by (7) to obtain

$$\left.\begin{aligned} B_{\mathrm{TE}}&=n\left[\frac{1}{2n^2}-\frac{1}{8}\frac{1}{n^4}\sin^2\theta_e+\ldots\right]\\ B_{\mathrm{TM}}&=\frac{1}{n}\left[\frac{1}{2n^2}-\frac{1}{8}\frac{1}{n^4}\sin^2\theta_e+\ldots\right]\end{aligned}\right\}. \tag{9}$$

These leading terms of B_{TE} and B_{TM} are independent of θ_e the fitting angle; for analytical purposes it may be convenient to choose the B's as

$$\left.\begin{aligned} B_{\mathrm{TE}}&=\frac{1}{2n}\\ B_{\mathrm{TM}}&=\frac{1}{2n^3}\end{aligned}\right\}. \tag{10}$$

This selection of B will be referred to as *normal matching* since it corresponds to improving the agreement of the reflection coefficients in the neighborhood of $\theta=0$, or normal incidence. The accuracy of this method is illustrated in graph 1a, where we

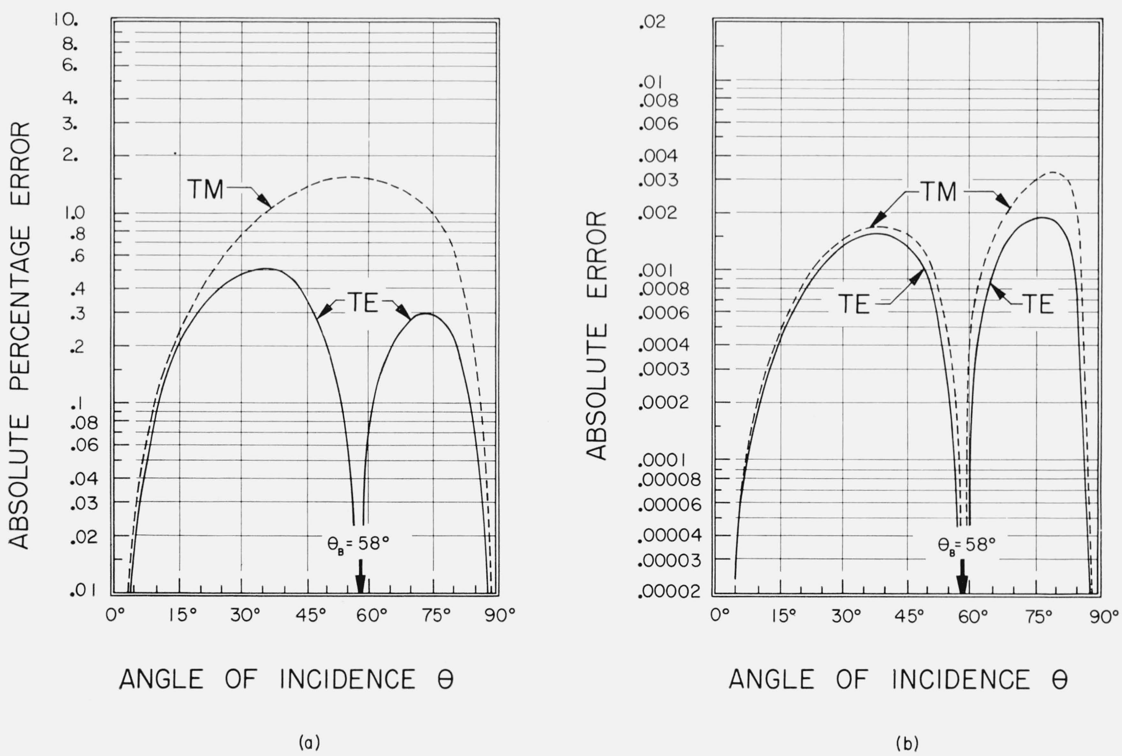

GRAPH No. 2.

The absolute percentage errors and the absolute errors that arise between the Fresnel reflection coefficients (5), (6) *and their approximations* (4) *plotted as a function of* θ *for the index of refraction* n=1.6.

In this case $B(\theta_e)$ has been chosen to make the match exact for Brewster's angle $\theta_e=\theta_b=\arctan n$, or for this case 58°.

plot the absolute percentage error [1] $\mathrm{PE}(\theta)$

$$\mathrm{PE}(\theta)=\left|\frac{R_A(\theta)-R_{\mathrm{TE,TM}}(\theta)}{R_{\mathrm{TE,TM}}(\theta)}\right|\times 100 \qquad (11)$$

between the reflection coefficients (5) and (6) and their approximations (4) with normal match coefficients for $n=1.6$. In the neighborhood of the Brewster's angle $\theta_B=\arctan n$, for which $R_{\mathrm{TM}}(\theta_B)=0$, the *percentage* error, *but not the absolute error*, for the TM approximation is necessarily unbounded. In graph 1b, we inspect the absolute error $\mathrm{AE}(\theta)$ as a function of θ for the same fitting

$$\mathrm{AE}(\theta)=|R_A(\theta)-R_{\mathrm{TE,TM}}(\theta)| \qquad (12)$$

and see that the absolute errors for both the TE and TM approximations have about the same values.

2.3. Brewster's Angle Matching

The unbounded percentage errors for the TM case in the vicinity of Brewster's angle can be eliminated by choosing $B_{\mathrm{TM}}(\theta_e)$ to yield a perfect match at Brewster's angle $\theta_e=\theta_B$, and (8) becomes

$$B_{\mathrm{TE,TM}}(\theta_B)=A_{\mathrm{TE,TM}}\frac{n^2+1}{n^2}\left\{1-\left[1-\frac{1}{n^2+1}\right]^{1/2}\right\} \qquad (13)$$

Graphs 2a and 2b illustrate the percentage and absolute errors for this choice of $B(\theta_B)$ for $n=1.6$. Notice the appreciable reduction in error as compared to the situation described by graph 1.

2.4. Chebyshev Matchings

Another choice for B is possible, at least for the TE approximation; this selection (fig. 2a) is a value of B_{TE} so chosen as to *minimize the maximum absolute percentage error* for the TE reflection coefficient. The magnitude of the error changes sign when the match is exact, i.e., at $\theta=\theta_e$. Suppose we vary θ_e until we obtain a value $\theta_e=\theta_T$ such that the maximum negative percentage error was the same magnitude as the maximum positive error. This balance will minimize the maximum absolute percentage error over the interval $-\pi/2\leq\theta\leq\pi/2$, by the Chebyshev criterion. The mathematical analysis to find the optimum Chebyshev matching would be interesting. Here we have done it by a trial and error process; the values of θ_T required to afford this match for the TE case are plotted in graph 3. The *maximum* associated errors for any real θ in the approximate reflection coefficient (4) are plotted in graph 4 as a function of n. It is not possible to repeat this procedure for the TM case due to the unbounded nature of the percentage error in the vicinity of Brewster's angle. However, a Chebyshev matching is feasible for both the TE and TM cases by minimizing the *absolute* error, but this was not analyzed.

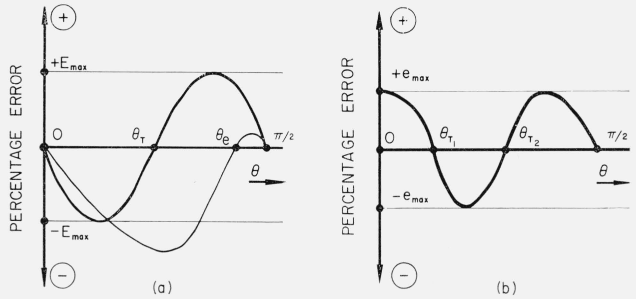

FIGURE 2. (a) *A Chebeyshev fitting is obtained when the fitting angle θ_e is so chosen that the maximum positive error, $+\mathrm{E}_{\max}$, equals the maximum negative error, $-\mathrm{E}_{\max}$.* (b) *A two-point Chebeyshev fitting can be obtained by sacrificing the demand for a perfect match at $\theta=0$.*

In case (b) the maximum error $e_{\max}$ would be less than the $E_{\max}$ of part (a).

Better Chebyshev fittings (fig. 2b) might arise by relaxing the demand of a perfect fit at $\theta=0$; this permits choosing both A_{TE} and B_{TE} to improve the match. This procedure would yield a perfect fit for *six* values of θ over the interval $-\pi/2\leq\theta\leq+\pi/2$. This particular matching was not carried out because of the labor involved in doing it empirically, and the excellent fit of the initial approximations.

2.5. Improved Angular Matchings

For other problems a useful procedure is to improve the approximation in the neighborhood of a specified angle of incidence. An example of a situation that would motivate this procedure is a transmitter T and distant receiver R both located near the earth's surface. The geometry is such that much of the energy collected by the receiver is associated with the arrival of rays in the neighborhood of grazing incidence. For this problem one might choose a value of B to match the *derivatives* [2] of the exact and the approximate reflections coefficient at grazing incidence; a simple calculation yields the result

$$B_{\mathrm{TE,TM}}(\pi/2)=A_{\mathrm{TE,TM}}\left\{1-\left[1-\frac{1}{n^2}\right]^{1/2}\right\}. \qquad (14)$$

---

[1] We inspect *errors* rather than compare actual and approximate curves since the two graphs would appear to coincide if superimposed.

[2] The values of these reflection coefficients themselves already agree for $\theta=\frac{\pi}{2}$.

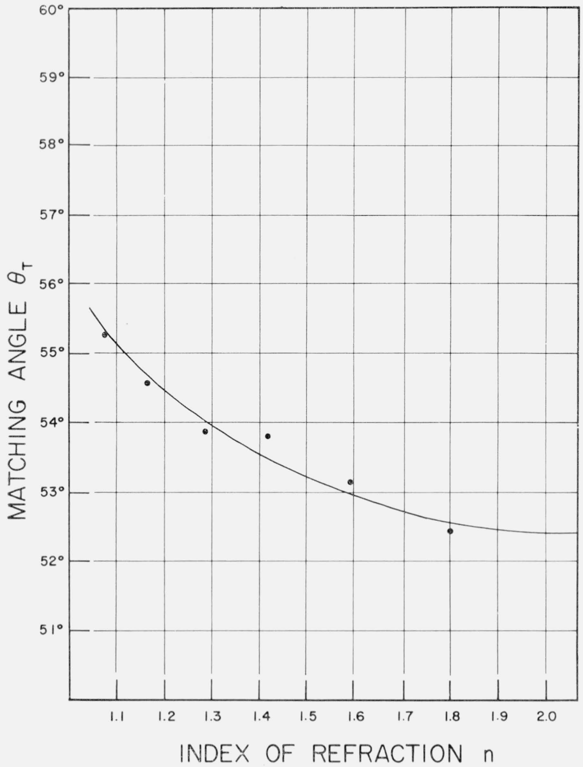

GRAPH No. 3.

The matching angle θ_T required to afford a Chebyshev fitting as a function of the index of refraction $n=\frac{k_2}{k_1}$.

The corresponding values of $B(\theta_T)$ are given by (8).

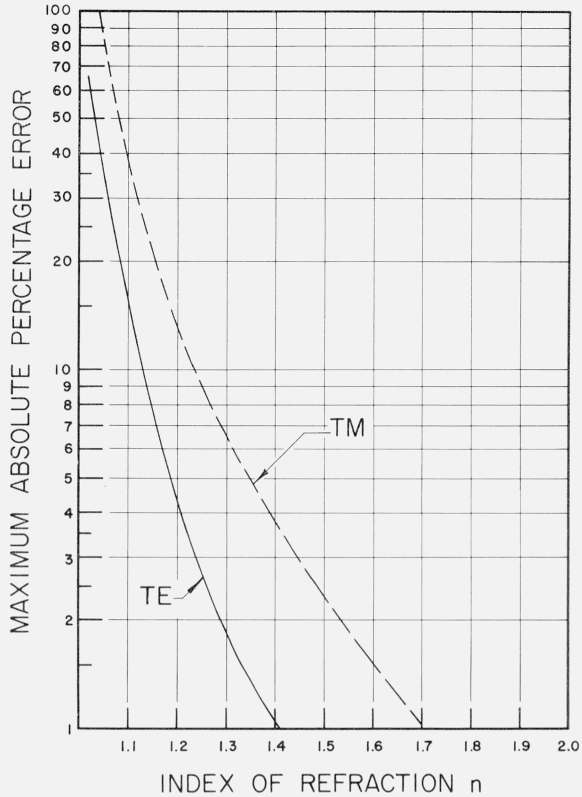

GRAPH No. 4.

The maximum absolute percentage errors that can arise in the approximate reflection coefficient for any real angle of incidence when the recommended matchings (TE-Chebyshev, TM-Brewster's angle) are chosen.

2.6. General Recommendations

Unless we wish to emphasize accuracy for a specified direction, it is reasonable to use the boundary condition (4) with Brewster's angle coefficients for problems of transverse magnetic excitation. For a problem of transverse electric excitation we would use the values of θ_T in curve (3) in formula (8) to yield a Chebyshev fit. The maximum percentage errors that arise for real angles of incidence for these two approximations are plotted for reference in graph 4 as a function of n, the index of refraction.

3. Generalizations

In addition to the above-mentioned methods, other refinements are possible. For example, any desired degree of accuracy can be obtained by adding additional terms to the boundary condition: an inclusion of additional terms proportional to

$$C\frac{\partial^4 u}{\partial x^4}, D\frac{\partial^6 u}{\partial x^6}, \dots$$

in the boundary condition (2) would have generated

$$R_A(\theta)=\frac{\cos\theta-(A+B\sin^2\theta+C\sin^4\theta+D\sin^6\theta+\dots)}{\cos\theta+(A+B\sin^2\theta+C\sin^4\theta+D\sin^6\theta+\dots)}$$

as the approximate reflection coefficient. The coefficients of these higher order terms would then be available to match either as many terms in a series expansion of the radical

$$\left[1-\frac{1}{n^2}\sin^2\theta\right]^{1/2}=A+B\sin^2\theta+C\sin^4\theta+D\sin^6\theta+\dots$$

as needed for extreme accuracy, or for use in more refined Chebyshev approximations.

From the preceding analysis, it is clear that the modeling of an interface by a linear boundary condition need not be restricted to dielectrics. The procedure can be used whenever the reflection coefficient from some arbitrary medium is given. For example, the reflection coefficient from an exponentially stratified medium is known [Wait, 1962b], and the present procedure can be repeated for that case. Such an analysis would be very interesting, and might be used, for example, to discuss ionospheric propagation from a day to a night region.

713-767—64——5

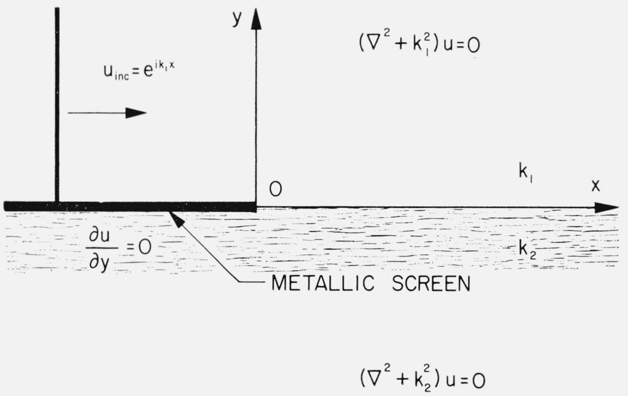

FIGURE 3. *The geometry of a test problem which serves to compare the use of the new boundary condition (2) with the use of the continuity of tangential $\vec{E}$ and $\vec{H}$ at a dielectric interface in a problem involving a horizontal discontinuity.*

4. Utility of the Boundary Condition in a Problem Involving a Horizontal Discontinuity

We have lent plausibility to a procedure which characterizes transition conditions at a dielectric interface by a linear boundary condition. This procedure is valid if the interface separates two half spaces, but what is its utility in a more complex geometry, say one for which there is a discontinuity in the horizontal direction? To answer this question, we have investigated a rigorously solvable test problem of the Wiener-Hopf type (cf, fig. 3). A plane wave is launched along a semi-infinite metallic screen located at the interface of two dielectrics. The termination of the screen produces a diffracted field that depends upon the physical parameters in a very complex fashion. It will be very significant if the new boundary condition implies results comparable to that obtained by a rigorous matching of tangential $\vec{E}$ and $\vec{H}$.

We obtain a reformulated version by removing the lower medium k_2 and replacing it by the new boundary condition (2) at $y=0$, $x>0$. The coefficients in this boundary condition are chosen to characterize the former transition conditions at the k_1-k_2 interface. We have indicated that there exists some flexibility in the choice of the parameters A and B; consequently, we shall leave them unspecified to see how various choices affect the diffracted field.

Let us specialize the discussion for the TM-case for which $H_x=H_y=0$, since this polarization allows a plane wave to propagate along a perfect conductor at grazing incidence. The importance of this fact is that if the plane wave travels in the positive x-direction, we can compare the diffracted fields for $x\to+\infty$, $y=0$ in both problems without the necessity of performing the *explicit* Wiener-Hopf decomposition. It would be of value to compare the fields in other directions, but that would involve a lengthy numerical program.

Let $u(x,y)=H_z$, then a standard approach [Kane and Karp, 1960], using dual integral equations, and Van der Waerden's saddle point analysis leads to the following asymptotic developments for $x\to+\infty$. For the exact problem, using matching conditions at the interface, we find for the far-field

$$\lim_{x\to+\infty} u(x,0) = -\left(\frac{k_2}{k_1}\right)^2 \left(\frac{2k_1}{k_2^2-k_1^2}\right)^{1/2} \frac{e^{i(k_1x-\pi/4)}}{(\pi x)^{1/2}} + 0(x^{-3/2}) \tag{15}$$

and likewise a corresponding result for the reformulated counterpart $u_A(x,y)$ using the linear boundary condition (2) along the positive x-axis

$$\lim_{x\to+\infty} u_A(x,0) = \frac{-(2k_1)^{1/2}}{A-B} \frac{e^{i(k_1x-\pi/4)}}{k_1(\pi x)^{1/2}} + 0(x^{-3/2}). \tag{16}$$

In both the rigorous (15) and the reformulated (16) asymptotic developments, the leading term in the diffracted field has canceled the incident plane wave. This is of course a consequence of the fact that the reflection coefficient for grazing incidence is -1 for either problem. It is more important to notice that for both problems, if $x>>1$, the *functional form of the leading terms (15) and (16) agree, and differ only by a numerical factor*

$$\frac{k_2^2}{k_1^2} \frac{1}{(k_2^2-k_1^2)^{1/2}} \leftrightarrows \frac{1}{k_1(A_{\rm TM}-B_{\rm TM})}$$

or, if we choose $A_{\rm TM}=1/n$,

$$\frac{n}{k_1\left(1-\frac{1}{n^2}\right)^{1/2}} \leftrightarrows \frac{1}{k_1\left(\frac{1}{n}-B_{\rm TM}\right)}.$$

The percentage error PE between these two coefficients is

$$\text{PE} = \left[1 - \frac{\left(1-\frac{1}{n^2}\right)^{1/2}}{1-nB_{\rm TM}}\right] \times 100, \tag{17}$$

and, by (9), $B_{\rm TM}$ is of the order $0(1/n^3)$ for fitting at any real angle, so that *this error decreases with increasing n.*

In line with the remarks in section 2.5, we observe that if in the far-field, the preferred direction had been chosen as grazing incidence, we would have used (14) to select a $B_{\rm TM}$ to match the derivative of the reflection coefficient at grazing incidence, i.e.,

$$B_{\rm TM} = \frac{1}{n}\left|1-\left(1-\frac{1}{n^2}\right)^{1/2}\right|. \tag{18}$$

For this choice there would have been *no error at all in (15) as compared with (16) for any n.*

We emphasize that the functional form of the leading terms in the diffracted field are the same for $y=0$, $x>>1$, but with differing coefficients for various choices of B_{TM}. For any selection of this parameter we can compute the percentage error (17) between the leading coefficients of (15) and (16). In graph 5, we plot three curves: (A) represents the "normal impedance" or Leontovich type approximation $\frac{1}{ik_1}\frac{\partial u}{\partial y}+A_{\mathrm{TM}}u=0$, obtained by setting $B_{\mathrm{TM}}=0$; (B) shows the error obtained by using the *normal match* values for B_{TM} given by (9). The smallness of the error in this case is significant because we are looking at the diffracted field in a direction perpendicular to that for which the coefficient B_{TM} was selected. The curve (C) illustrates the error if B_{TM} is chosen as indicated by (13) which is a matching at Brewster's angle. We obtain the expected improvement over case (B) since Brewster's angle is closer to grazing incidence than normal incidence. Notice that the big improvement is from (A) to (B), *a correction which arises from the additional term in the boundary condition.*

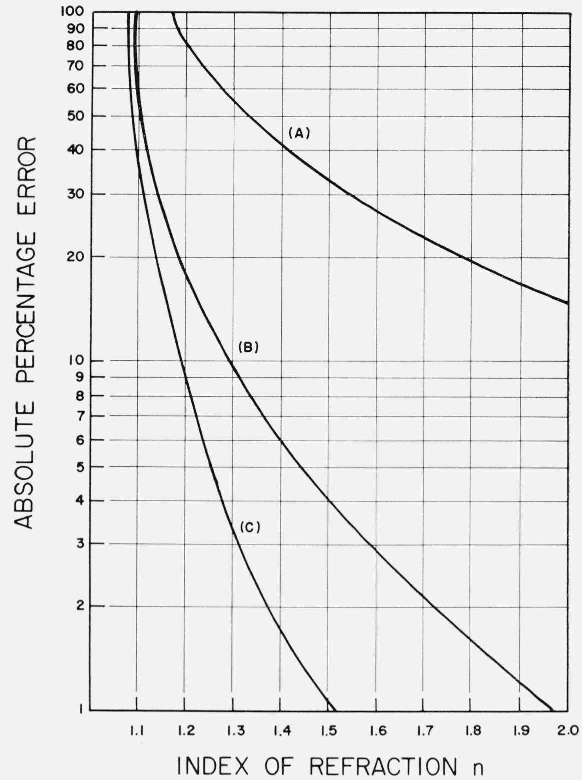

GRAPH No. 5.

A comparison of the errors that arise for $x>>1, y=0$ *in the total field including diffraction effects of the test problem involving a horizontal discontinuity.*

5. Concluding Remarks

5.1. Reciprocity

A feature of the new boundary condition (2) is that it involves a second derivative. This somewhat surprising detail has been inserted to guarantee reciprocity. A first derivative could have been used, but it would not lead to reciprocal phenomena. This point can be most easily established by an inspection of the associated reflection coefficient. If the boundary condition had been written with a single x-derivative

$$\frac{1}{ik_1}\frac{\partial u}{\partial y}+Au+\frac{B}{k_1}\frac{\partial u}{\partial x}=0$$

its reflection coefficient would have been

$$R_A(\theta)=\frac{\cos\theta-(A-B\sin\theta)}{\cos\theta+(A-B\sin\theta)}$$

which is *not* the same for a wave reflected from the left as compared to one reflected from the right since $\sin\theta$ changes sign with θ.

5.2. Existence and Uniqueness

That solutions of problems involving the new boundary condition do exist can readily be shown by construction [Kane and Karp, 1960; Jones, 1962]. In addition these references illustrate the use of the boundary condition, and also its ability to reproduce complex diffraction phenomena. In addition, the uniqueness has also been established [Kane, 1961].

5.3. Limitations

The approximation procedure is limited by the restriction $k_2>k_1$, or $n>1$. For, if $k_2<k_1$, there arises a real angle of incidence corresponding to total reflection at which the second radical in (5) and (6) becomes imaginary. Since (4) involves constant coefficients, the boundary condition is unable to imitate a transition from a real reflection coefficient to a complex one for *real* angles of incidence. This is clear by inspection of the reflection coefficient (4); so long as both A and B are real, the reflection coefficient remains real for any real angle θ.

Observe, from graph 5, that the approximation deteriorates for $n\approx 1$. Physically $n\approx 1$ corresponds to an interface with a vanishing reflection coefficient, which is difficult to approximate on a percentage basis.[4] However, *the absolute errors remain small and bounded.* As a consequence the boundary condition (4) specialized for $n=1$ may be useful as a model of a perfect absorber since the reflection coefficient it defines is so small. A curve of this special $R_A(\theta)$ is drawn in graph 6. We see that $R(\theta)\approx 0$ until $|\theta|=60°$; it is unavoidable that $R(\theta)\rightarrow -1$ for $|\theta|\rightarrow\frac{\pi}{2}$; this is so even for the exact reflection coefficient if $n\neq 1$.

[4] However this fact allows one to use other approximate methods [Karp and Sollfrey, 1950].

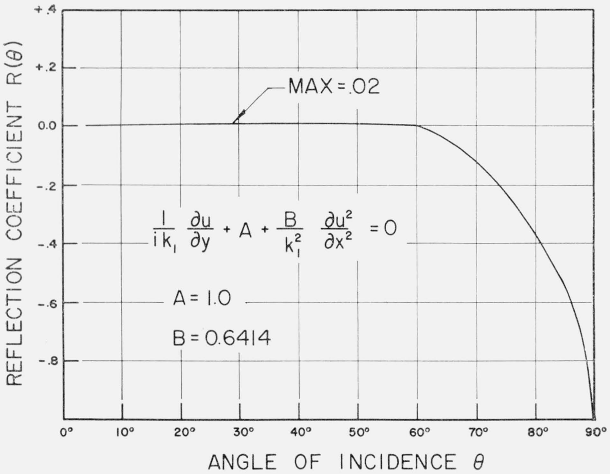

Graph No. 6.

A special boundary condition which defines an almost vanishing reflection coefficient for $0 \leq |\theta| \leq 60°$, *indicating that the boundary condition may be used as a model of a perfect absorber. It is unavoidable that* $R(\theta) \rightarrow -1$ *for* $|\theta| = \pi/2$; *this is forced by the form of the reflection coefficient (2.8).*

6. References

Brekhovskikh, L. M. (1960), Waves in Layered Media (Academic Press, New York, N.Y.).

Grünberg, G. A. (1943), Suggestions for a theory of costal refraction, Phys. Rev. **63,** 185–189.

Jones, W. R. (1962), An approximate approach to problems involving surface waves, Hughes Research Report FL62–1, Hughes Aircraft Co., Culver City, Calif.

Kane, J., and S. N. Karp (1960), Radio propagation past a pair of dielectric interfaces, New York University Research Report EM–154, New York, N.Y.

Kane, J. (Dec. 1961), A uniqueness theorem for the reduced wave equation, Proc. Am. Math. Soc. **12,** 967.

Karp, S. N , and W. Sollfrey (1950), Diffraction by a dielectric wedge, New York University, Inst. Math. Sci. Div. Em Res., Research Report No. EM–23.

Leontovich, M. A. (1944), A method for the solution of the problem of the propagation of electromagnetic waves along the surface of the earth, Izvest. Akad. Nauk SSSR, Ser. Fiz **8,** 16. (A more accessible reference can be found in Brekhovskikh above.)

Stratton, J. A. (1941), Electromagnetic Theory (McGraw-Hill Book Co., Inc., New York, N.Y.).

Wait, J. R. (1962a), The propagation of electromagnetic waves along the earth's surface, Electromagnetic Waves, Ed. R. E. Langer (The University of Wisconsin Press, Madison, Wis.).

Wait, J. R. (1962b), Electromagnetic Waves in Stratified Media (Pergamon Press Ltd., Oxford, London).

(Paper 68D3–346)